Kinetic parameter estimation in *N. europaea* biofilms using a 2-D reactive transport model

Authors: Ellen G. Lauchnor, Lewis Semprini, & Brian D. Wood

Lauchnor EG, Semprini L, Wood BD, "Kinetic parameter estimation in N. europaea biofilms using a 2-D reactive transport model," Biotechnology and Bioengineering 2015 112(6): 1122–1131.

Kinetic Parameter Estimation in N. europaea Biofilms Using a 2-D Reactive Transport Model

Ellen G. Lauchnor,[1] Lewis Semprini,[2] Brian D. Wood[2]

[1] Center for Biofilm Engineering, Montana State University, 366 EPS, Bozeman 59717, Montana; telephone: 406-994-2134

[2] School of Chemical, Biological and Environmental Engineering 102 Gleeson Hall, Oregon State University, Corvallis 97331, Oregon

Abstract:

Biofilms of the ammonia oxidizing bacterium *Nitrosomonas europaea* were cultivated to study microbial processes associated with ammonia oxidation in pure culture. We explored the hypothesis that the kinetic parameters of ammonia oxidation in N. europaea biofilms were in the range of those determined with batch suspended cells. Oxygen and pH microelectrodes were used to measure dissolved oxygen (DO) concentrations and pH above and inside biofilms and reactive transport modeling was performed to simulate the measured DO and pH profiles. A two dimensional (2-D) model was used to simulate advection parallel to the biofilm surface and diffusion through the overlying fluid while reaction and diffusion were simulated in the biofilm. Three experimental studies of microsensor measurements were performed with biofilms: i) NH_3 concentrations near the K_{sn} value of 40mM determined in suspended cell tests ii) Limited buffering capacity which resulted in a pH gradient within the biofilms and iii) NH_3 concentrations well below the K_{sn} value. Very good fits to the DO concentration profiles both in the fluid above and in the biofilms were achieved using the 2-D model. The modeling study revealed that the half-saturation coefficient for NH_3 in N. europaea biofilms was close to the value measured in suspended cells. However, the third study of biofilms with low availability of NH_3 deviated from the model prediction. The model also predicted shifts in the DO profiles and the gradient in pH that resulted for the case of limited buffering capacity. The results illustrate the importance of incorporating both key transport and chemical processes in a biofilm reactive transport model.

KEYWORDS: ammonia oxidizing bacteria; biofilm model; microbial kinetics; Nitrosomonas europaea

Introduction:

Kinetic parameters in biofilms are difficult to determine experimentally due to mass transfer limitations that result in gradients of substrates and heterogeneous activity within a biofilm (Riefler and Smets 2003). Reactive transport modeling is a very useful tool for simulating microbial reaction rates within biofilms (Bernet et al., 2005; Masic et al., 2010). The kinetic parameters determined for enzymatic reactions in batch or suspended systems of an organism or consortium are sometimes used to represent the kinetics of those reactions in biofilms (Bernet et al., 2005; Mirpuri et al., 1997; Park et al., 2010). However, phenotypic and physiological differences between suspended and biofilm cells have been observed and can influence metabolic reactions (Costerton et al., 1999; Lazazzera 2005; Monds and O'Toole 2009; Stewart and Franklin 2008). More research on autotrophic bacteria is needed to confirm that the modeled reaction kinetics in suspended cells can be applied to biofilms. Particularly, the enzymatic reaction catalyzing ammonia oxidation may be influenced by biofilm formation due to different levels of enzyme production during biofilm growth and maintenance. In this work, we examined kinetics of ammonia oxidation in both suspended cultures and biofilms of the ammonia oxidizing bacterium, *Nitrosomonas europaea* by comparing direct measurements to simulations using a reactive transport model.

Ammonia oxidizing bacteria (AOB) are a group of bacteria that oxidize ammonia to nitrite, the first step of nitrification. *N. europaea* is an AOB that has been well-characterized in pure cultures of suspended cells (Arp et al., 2002), making it an ideal model AOB for kinetic studies. To effectively model nitrifying biofilms, the kinetic parameters for ammonia oxidation must be evaluated in a biofilm. It should be noted that N. europaea oxidizes NH3 and not NH4+, thus the pH dependent speciation of ammonia must be incorporated into a reactive transport model.

Biofilm kinetics have been evaluated using models that correlate bulk measurements of microbial activity to reaction and diffusive mass transport (Park and Bae 2009; Perez et al., 2005). However, the use of microelectrodes allows for spatially resolved measurement of species, such as dissolved oxygen (DO) and pH, inside of biofilms (Gieseke and deBeer 2004; Revsbech and Jorgensen 1986). Microelectrodes have been used to measure concentration profiles

in nitrifying biofilms to determine rates of nitrifying activity (Gieseke et al., 2003; Okabe et al., 1999; Okabe et al., 2002) and kinetic parameters (Schramm et al., 1999); and to evaluate kinetic parameters in biofilms without consideration of transport and fluid flow effects (Yurt et al., 2003; Zhou et al., 2008). The concentration profiles can also be used as direct measurements for model calibration (Masic et al., 2010; Yurt et al., 2003). The model developed here includes both diffusive and advective transport of solutes and reaction kinetics within the biofilm.

Fluid flow has been incorporated into some biofilm models, and thus transport occurs in two directions, with the fluid flow (parallel to the biofilm surface) and by diffusion into the biofilm; thus a 2-D geometry is often required for modeling the advective transport of species between an overlying fluid phase and the biofilm (Eberl and Sudarsan 2008). A reactive transport model (RTM) used to evaluate biofilm kinetics must incorporate (i) the effect of advective transport in the fluid phase, (ii) the diffusive mass transfer from the fluid phase to the biofilm, and (iii) diffusive transport within the biofilm.

The research presented here uses microelectrode measurements and a 2-D reactive transport model to evaluate the kinetics of ammonia oxidation in pure culture biofilms of *N. europaea*. The goals of this research were to: develop a 2-D RTM simulating autotrophic AOB biofilms that included mass transport both in the fluid and the biofilm and aqueous species equilibria; and evaluate the kinetic parameters for NH_3 oxidation by *N. europaea* in biofilms by calibrating the model with experimental pH and DO measurements in the biofilms. Such a study has not been previously performed with a pure culture nitrifying biofilm. Three studies that integrated experimental microsensor measurements and modeling were conducted to achieve these goals. In Study I, microelectrode experiments under buffered conditions were performed at varying concentrations of NH_3 to evaluate kinetics and transport. In Study II, pH buffer concentration was reduced to explore the effect of pH gradients inside the biofilm on microbial kinetics. Finally, for Study III the affinity of biofilm cells towards NH_3 was determined by evaluating the kinetics of NH_3 oxidation under NH_3 limited conditions.

Experimental Procedures

Bacterial Cultures

Batch cultures of *N. europaea* cells (ATCC strain 19718) were grown for biofilm reactor inoculation and suspended batch tests. Cell cultivation was performed in 4-L flasks containing 2 L of medium as described previously (Radniecki et al., 2008). The flasks were inoculated with 25 mL of *N. europaea* culture and shaken (100 RPM) at 30°C in the dark and cells were harvested upon reaching late exponential phase on day 3 ($OD_{600} = 0.07$).

Batch Tests

For batch tests, *N. europaea* cultures were harvested in late exponential phase, centrifuged at 9000 RPM and suspended in 30 mM HEPES buffer adjusted to pH 7.8 with NaOH. Cells were added to 155 mL Wheaton bottles with septa caps containing 50 mL of medium and the final cell concentration was 6 mg protein L^{-1}. The bottles were shaken (200–250 RPM) for 3 h at 30°C and NO_2^- production was monitored by extracting liquid samples at 30-min intervals and performing a colorimetric assay for NO_2^- (Hyman and Arp 1995).

Biofilm Reactor

A drip flow biofilm reactor (DFR) was used to cultivate biofilms of *N. europaea* according to standard methods developed (Goeres et al., 2009) with some modifications to the pumping rate and medium composition (Lauchnor et al., 2011). Details on the DFR operation and a schematic can be found in the Supporting Information (Fig. S1).

Oxygen and pH Microsensor Measurements

After being cultivated to steady-state, determined by levels of NO_2^- production, mature biofilm samples on glass slide coupons (7.5 cm x 2.5 cm) were removed from the DFR channels (10.16 cm × 2.55 cm) for microsensor measurements. The coupon containing the biofilm was placed inside a flow cell connected to a 5 L media reservoir maintained at 25°C with a recirculating heater and open to the atmosphere (Table SI and Fig. S2). The media from the reservoir was recirculated through the flow cell at a flow rate of 50 mL min^{-1}. The media reservoir was continuously sparged with air to ensure a constant concentration of dissolved O_2 at the saturation value.

Oxygen microsensors (OX-10) and pH microelectrodes (pH-10) with tip diameters of 8–12 μm (Unisense, AS, Denmark) were used to take vertical concentration profiles within the biofilms. A micromanipulator with motor controller (Marzhauser, Germany) was used for positioning the microelectrodes relative to the biofilm surface and making vertical spatial steps (20–25 μm) while profiling. Each vertical profile was initiated in the bulk fluid starting 1000 μm above the biofilm. Data acquisition was performed on a laptop computer using the SensorTrace Pro software (Unisense, AS). Additional information on microelectrode methods can be found in the Supporting Information.

Biofilm depth and coverage on the slides was heterogeneous, with the depth varying between 0–300 μm. Locations on the slide for microelectrode measurements were found using the Stereomicroscope where the biofilm was at least 200–300 μm in depth. All locations used for microelectrode experiments were roughly along the center line of the coupon (in direction of flow) and within 2 cm of the influent edge of the coupon. Three to five replicate profiles were taken for each experimental condition tested.

Experimental Conditions

The liquid medium for microsensor experiments contained HEPES buffer (1 or 10 mM) at pH 7.8. Atmospheric DO at 25°C was 258 μM, which provides the stoichiometric equivalent for oxidation of 172 μM NH_3. Ammonium was added as aliquots from a 0.5 M $(NH_4)_2SO_4$ stock solution to the media bath and the fluid was recirculated into the flow cell for at least 1 h to ensure well-mixed conditions. Increasing concentrations of $(NH_4)_2SO_4$ were added to

the bath in order to compare DO profiles under different conditions on the same biofilm samples.

The experimental conditions for the three microsensor studies are outlined in Table I. Each study was conducted under steady-state conditions; which were ascertained by taking multiple measurements over time to verify that there were no changes in the concentration profiles.

Model Development

Batch Model

The COMSOL version 4.1 Reaction Engineering Module was used to create a transient kinetic model of NH_3 oxidation in a batch system in the absence of mass transport. Acid-base equilibrium equations as well as the Monod rate equation for ammonia oxidation were included to describe the chemistry in the batch system. Biomass [X] was specified as a constant because cell concentration did not change over the 2 h tests. The data from the short term batch experiments describe above were imported into the COMSOL model to calibrate the kinetic parameters k_{max} and K_{sn}. The batch model was also used to evaluate the model performance with the addition of buffering and pH change.

2-D Model Equations

A 2-D biofilm model was developed with fluid and biofilm subdomains (Fig. 1). The biofilm geometry was a flat surface with a uniform depth of 300 μm, which was the approximate maximum measurement determined by microscopic examination of the biofilms. In the biofilm model, growth and detachment of biofilm biomass was ignored due to the short-term duration of experiments. Conservation of mass equations were solved for chemical species involved in the reactions for AOB respiration and equilibrium aqueous chemistry.

The mass balance equation for the fluid subdomain contained both advective and diffusive transport of solutes at steady-state, as follows:

$$u_x \frac{\partial C}{\partial x} = D_i \left(\frac{\partial^2 C}{\partial x^2} + \frac{\partial^2 C}{\partial y^2} \right) \quad (1)$$

In equation 1, u_x is the fluid velocity in the x-direction, D_i is the diffusion coefficient (Table II) and no reaction in the fluid is assumed. Steady-state conditions were verified by repeated profile measurements, which showed no change with time. The solution for the fluid velocity field was generated from the Navier-Stokes equation, assuming laminar flow in only the x-direction close to a flat surface with no flow at the surface and an upper boundary of maximum velocity, u_{max}.

$$u_x(y) = \frac{u_{max}}{D^2} * (2dy - y^2) \quad (2)$$

$$u_{max} = \frac{Q_T}{A_{inlet}} = \frac{Q_T}{\left(\pi \frac{w^2}{4}\right)} \quad (3)$$

In equation 2, d is the depth above the biofilm at which the fluid velocity is equal to the maximum fluid velocity, u_{max}. In equation 3, total flow rate is Q_T, the cross sectional area of the flow cell inlet is A_{inlet} and w is the diameter of the inlet port. The resulting velocity profile is parabolic with $u_x(y = 0) = 0$ at the biofilm surface and $u_x(y = d) = u_{max}$. The slide was positioned more than 2 cm downstream of the inlet port and a mesh screen was placed upstream of the slide to diffuse the flow, thus the velocity profile was assumed to be fully developed at the biofilm.

In the biofilm it was assumed that solute transport was solely by diffusion, thus the following steady-state mass balance equation in 2-D for a reacting solute in the biofilm was used:

$$R = D_{eff} \left(\frac{\partial^2 C}{\partial x^2} + \frac{\partial^2 C}{\partial y^2} \right) \quad (4)$$

R is the reaction rate of species C and D_{eff} is the diffusion coefficient in the biofilm. In equation 4, the effective diffusion coefficient of species i in the biofilm, $D_{eff,i}$, is equal to the diffusion coefficient in water, D_i, multiplied by an effectiveness factor to account for diffusive resistance due to the cell matrix (Wood et al., 2001). Following (Wood et al., 2002), we used a value of 0.8 for all species to correct for effective diffusion D_{eff}. A sensitivity analysis of the effective diffusivity (SI and Fig. S3) indicated that no observable difference was found between effectiveness factors of 0.7 and 1 in the biofilm.

To describe R for each species the reaction rates in Table III were calculated and the stoichiometry of the species in the table was multiplied by the reaction rates to determine the net change in species. The oxidation of NH_3 to NO_2^- by *N. europaea* was modeled according to the following reaction: $NH_4^+ + 1.5O_2 \rightarrow NO_2^- + 2H^+ + H_2O$ (Tarre and Green 2004). The kinetic model typically used for NH_3 oxidation is the Monod equation with dual substrate dependence on NH_3 and O_2 (Downing and Nerenberg 2008; Park et al., 2010; Perez et al., 2009).

$$R_{AOB} = k_{max} X \frac{NH_3}{K_{sn} + NH_3} \frac{O_2}{K_{so} + O_2} \quad (5)$$

In equation 5, k_{max} is the maximum rate coefficient, while K_{sn} and K_{so} are half-saturation coefficients for NH_3 and O_2, respectively.

Table I. Experimental conditions for microsensor measurements.

	Study I – kinetic evaluation	Study II – pH gradient	Study III – NH_3 limitation
NH_4-T (mmol L^{-1})	0, 1, 5, 5 + ATU	0.5, 1.5, 5	0, 0.05, 0.1, 0.25, 5
Initial NH_3 (mmol L^{-1})	0, 0.034, 0.171	0.017, 0.051, 0.171	0, 0.0017, 0.0034, 0.0086, 0.171
HEPES buffer (mmol L^{-1})	10	1	10
Biofilm age (days cultivated)	42	51	49

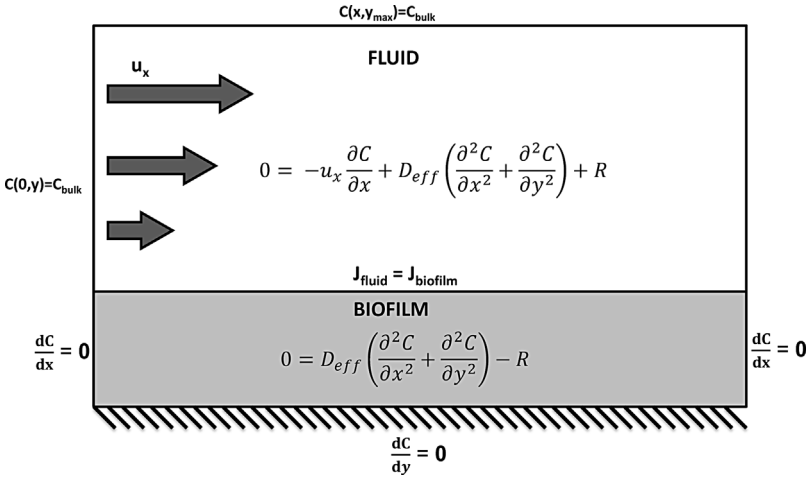

Figure 1. Model of 2-D reaction and transport in biofilm.

Endogenous respiration was included, where the decay coefficient, *b*, of 0.15 d^{-1} was estimated from DO profiles taken with no NH_3 present (SI, Fig. S4) and multiplied by a yield, *Y*, of 2.1 mg protein per mmol O_2 (Rittmann and McCarty 2001).

The aqueous chemistry of the system and acid-base equilibria were taken into account to determine the fraction of total ammonium species (NH_4-T) that is available as free $NH_{3(aq)}$ for microbial reaction and to model the pH in the system as a function of HEPES buffering capacity. To incorporate the acid-base equilibria in the RTM, the equilibrium reactions were represented as reversible reactions with high rate constants.

$$K_{aN} = \frac{k_1}{k_2} = \frac{NH_3 * H^+}{NH_4^+} \quad (6)$$

$$R_{eq} = k_2\left[K_{aN} * NH_4^+ - NH_3 * H^+\right] \quad (7)$$

Three equations in the form of equation 6 were used to account for equilibria of NH_3/NH_4^+, HEPES acid/base, and H_2CO_3/HCO_3^- (Table II and III). A bulk fluid concentration of 10^{-5} mol L^{-1} H_2CO_3 was used to simulate equilibrium with atmospheric CO_2. The

Table II. Physical constants and kinetic parameters for the biofilm model.

		Value	Units	Source
Parameter				
Flow rate	Q_T	50	mL min^{-1}	Measured
Inlet width	w	0.5	cm	Measured
Fluid height above biofilm at v_{max}	d	1.0	cm	Measured
Diffusion coefficients				
Ammonium	D_{NH4+}	1.96e-5	cm^2 s^{-1}	[Kreft et al., 2001]
Ammonia	D_{NH3}	1.64e-5	cm^2 s^{-1}	[Cussler 1997]
Oxygen	D_{O2}	2.0e-5	cm^2 s^{-1}	[Cussler 1997]
Nitrite	D_{NO2-}	1.7e-5	cm^2 s^{-1}	[Kreft et al., 2001]
Protons	D_{H+}	9.3e-5	cm^2 s^{-1}	[Robinson and Stokes 1959]
HEPES	D_{HEPES}	6.2e-6	cm^2 s^{-1}	[Robinson and Stokes 1959]
HCO_3^-/H_2CO_3	D	7.5e-6	cm^2 s^{-1}	[Robinson and Stokes 1959]
Acid-Base Equilibrium Constants				
NH_3/NH_4^+	K_{aN}	$10^{-9.25}$	mol L^{-1}	[Lide 2007]
HEPES Acid/Base	K_{aH}	$10^{-7.8}$	mol L^{-1}	[Lide 2007]
HCO_3^-/H_2CO_3	K_{aDIC}	$10^{-6.3}$	mol L^{-1}	[Lide 2007]
Kinetic parameters				
Half-saturation for O_2	K_{so}	15.6	μmol L^{-1}	[Rittmann and McCarty 2001]
Half-saturation for NH_3	K_{sn}	4–40	μmol L^{-1}	Fitted in studies 1, 2
Maximum rate	k_{max}	0.005	μmol mg $prot.^{-1}$ s^{-1}	Fitted in study 1
	k_2	10^6		
Endogenous decay	b	8.2e-5	μmol mg $prot.^{-1}$ s^{-1}	Fitted
Effective diffusivity	*eff*	0.8	–	[Wood et al., 2002]

Table III. Kinetic and equilibrium rate expressions.

Reaction	Expression	NH_3	NH_4^+	NO_2^-	H^+	O_2	HEPES base	HEPES acid	H_2CO_3	HCO_3^-
Ammonia oxidation	$\frac{K_{max}XNH_3}{K_{sn}+NH_3}\frac{O_2}{K_{so}O_2}$	−1	–	1	2	−1.5	–	–	–	–
NH_3/NH_4^+ equilibrium	$k_2[K_aNH_4^+ - NH_3H^+]$	1	−1	–	1	–	–	–	–	–
HEPES buffer equilibrium	$k_2[K_aHEPES_{acid} - HEPE]$	–	–	–	1	–	1	−1	–	–
Bicarbonate equilibrium	$k_2\left[K_aH_2CO_3 - HCO_3^-H^+\right]$	–	–	–	1	–	–	–	−1	1
Endogenous respiration	bX	–	–	–	–	−1	–	–	–	–

equilibria between species were verified in the model solution by comparing the right side of equation 6 with the equilibrium constants.

In Figure 1, the boundary conditions for each species are shown in addition to the model mass balance equations. At the effluent, diffusive flux is negligible in the direction of flow, which is validated by the magnitude of diffusion coefficients for the species (Table II).

Model Solution

The RTM was solved using the COMSOL 4.1 Multiphysics package with the Chemical Reaction Engineering module. COMSOL uses a finite element method to solve the PDEs describing the species concentrations at each model node. The computational grid was 200 nodes in the x-direction (fluid flow), and in the y-direction there were 40 nodes in the fluid and 30 nodes in the biofilm domain. A transient solver was used to iteratively solve for all chemical species until arriving at the steady-state solution.

The model solution for the fluid flow equation was verified by comparison with the analytical solution for the velocity field (equation 2). The model solution for chemical species was verified by performing mass balances on nitrogen species in the system, to confirm that the modeled reactions resulted in stoichiometric changes in product (NO_2^-) and reactants (NH_3, O_2).

Least Squares Method

For the 2-D biofilm model calibration, a least-squares error method was used for comparison of experimental data and model prediction of the oxygen profiles in the biofilms to determine the best fit kinetic parameters, K_{sn} and k_{max}. The parameter fitting was done manually for each parameter with a range of parameter values, until a minimum value for the sum of squared error was found to two significant figures.

Results And Discussion

Batch Experiments—Suspended Cell Kinetic Parameters

Short term experiments and a batch model were used to simulate NH_3 oxidation kinetics with suspended cells. The Monod term for oxygen in equation (5) was assumed to be ~ 1 ($[O_2] >> K_{so}$), because the reactors were well shaken with adequate headspace. In medium containing 5 mmol L^{-1} NH_4-T, the rate of NO_2^- production over 30 min determined by linear regression was 0.05 μmol mg protein^{-1} s^{-1}. This value was used as k_{max} in the batch model (Fig. 2). This parameter is within the range of maximum NH_3 oxidation rates from previous studies, which vary from 0.023 μmol mg protein^{-1} s^{-1} (Radniecki et al., 2008) to 0.096 μmol mg protein^{-1} s^{-1} (Keener and Arp 1993). Although nitrite accumulation at or above 5 mM can inhibit AOB (Stein and Arp 1998), this

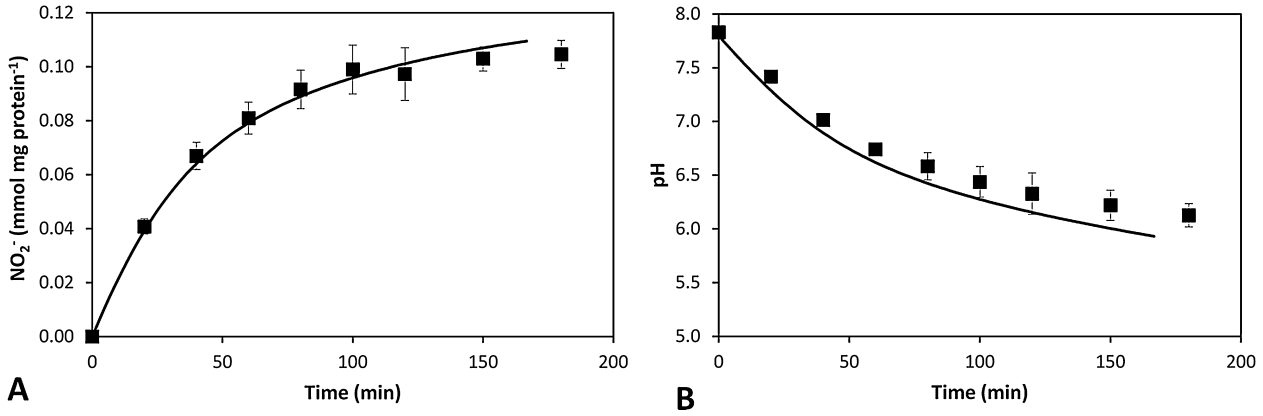

Figure 2. Results of nitrite production and pH change in batch experiments conducted with 5 mM NH_4-T and compared to the batch Reaction Engineering COMSOL model. (**A**) Nitrite accumulation over time (**B**) pH decrease over time due to ammonia oxidation. Data points are averages of triplicate experiments (■) and lines are model simulations with optimized kinetic parameters. Error bars represent standard deviations of experiments.

was not considered in the model. The Monod rate equation used to model ammonia oxidation did not consider pH dependence of either the kinetic parameters or nitrite inhibition, but these terms can be added in further studies. The batch COMSOL model was able to accurately simulate the nitrite production rate in the batch system using a K_{sn} value of 40 μM NH_3 (Fig. 2A). These results agree with a previous study that experimentally determined the K_{sn} value to be 23–58 μM NH_3 for *N. europaea* (Suzuki et al., 1974). Using pH data from the same batch experiment, the pH shift during NH_3 oxidation was modeled (Fig. 2B). The pH data was best simulated when both carbonate and HEPES equilibrium equations were included in the batch model (Fig. 2B). The reduction in NO_2^- production rate over time was a result of a combined effect of ammonia depletion and the pH decrease that additionally limits the NH_3 available to AOB.

Study I – Biofilm Kinetics of Ammonia Oxidation

DO profiles were taken in biofilms submerged in the flow cell with media containing 0, 1 and 5 mmol L^{-1} NH_4-T (Fig. 3A). DO consumption increased from the 1 mmol L^{-1} to 5 mmol L^{-1} NH_4-T, as evidenced by the steeper slope and lower DO concentration in the 5 mmol L^{-1} profile. This indicated that with 1 mmol L^{-1} NH_4-T, NH_3 was at or below K_{sn} for at least some of the biofilm cells. At a NH_4-T concentration of 1 mM, the NH_3 species concentration is 34 μM, which is similar to the K_{sn} value, or half saturation constant of 40 μM determined in the batch system, indicating that batch cells at this concentration would oxidize NH_3 at half of the maximum rate observed at 5 mM NH_4-T.

Allylthiourea (ATU), a specific inhibitor of AMO, was added to the water bath to a final concentration of 100 μM with 5 mmol L^{-1} NH_4-T present. Upon ATU addition, NH_3 oxidation ceased and O_2 increased in the biofilms as it was no longer being consumed for ammonia oxidation. The response to ATU was rapid and the dissolved O_2 at the biofilm surface returned to 90% of atmospheric DO concentration within 10 min of ATU addition. After addition of ATU, a slight decline in DO inside the biofilms was observed (Fig. 3A) indicating endogenous respiration in the absence of NH_3 oxidation, which was fitted to a model profile by calibrating the endogenous decay constant (b) in Figure S4.

The pH was between 7.6 and 7.8 throughout the fluid and biofilm (SI, Fig. S5). The excess buffering capacity of 10 mM HEPES prevented the H^+ produced during NH_3 oxidation from causing a pH drop in the biofilm. This allowed for evaluation of AOB biofilm kinetics without pH gradients impacting NH_3 availability.

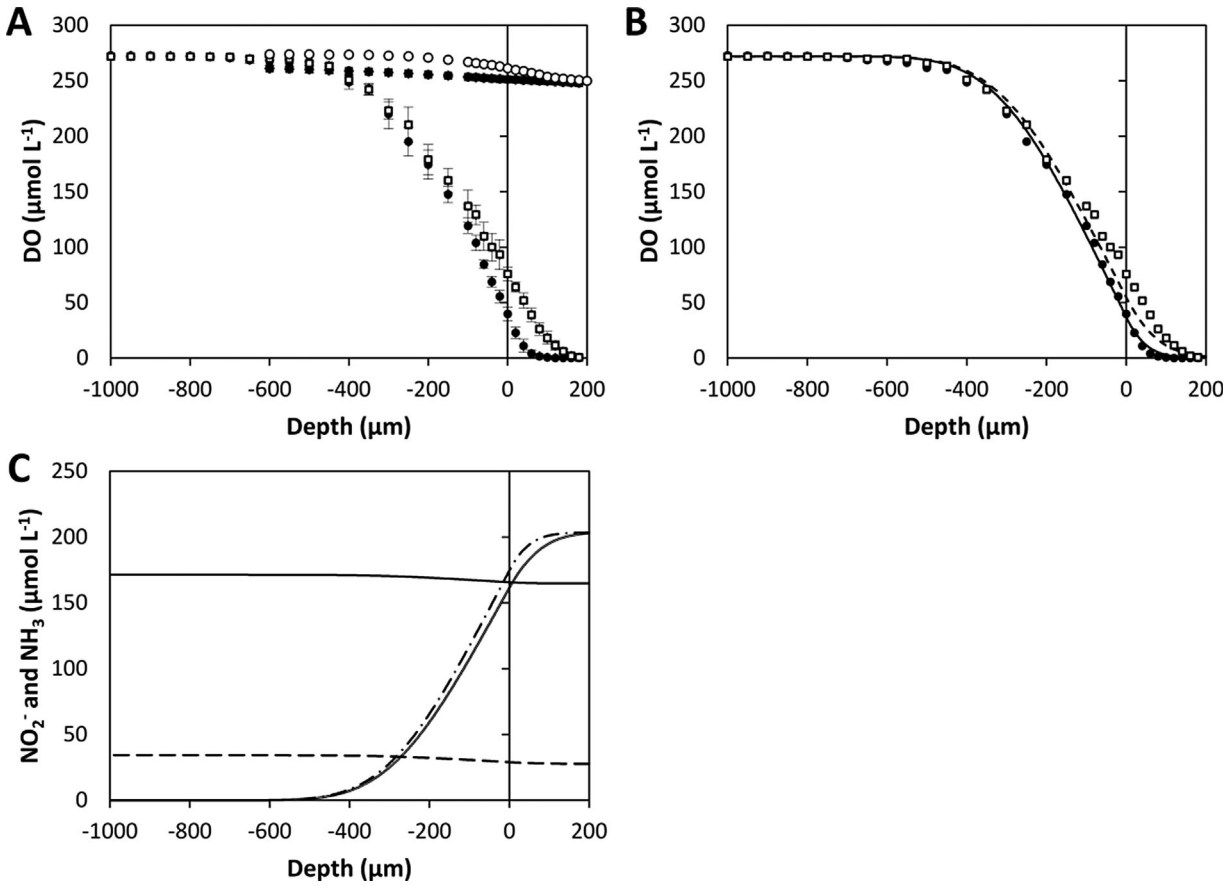

Figure 3. 1-D vertical profiles of DO, NH_3 and NO_2^- from Study 1 at a location 2 cm from the inlet. **A)** Measured DO in the presence of various NH_4-T concentrations: 0 mmol L^{-1} (■), 1 mmol L^{-1} (□), 5 mmol L^{-1} (●), 5 mmol L^{-1} after addition of ATU (○) **B)** Model fit to DO measurements at the same location by optimization of maximum rate where K_{sn} = 40 μM NH_3 and $k_{max}X$ = 0.025 mol L^{-1} s^{-1} **C)** Modeled NH_3 and NO_2^- concentrations at the same location. Lines represent model solutions at NH_4-T concentrations of 1 mM (dashed line) and 5 mM (solid line), using a K_{sn} of 40 μM NH_3 and biomass concentration of 5,000 mg protein L^{-1}. Error bars represent standard deviation of triplicate profiles.

Biomass concentration [X] was estimated from experimental measurements. It is difficult to obtain exact values for [X] in a biofilm, which often requires microscopic methods to evaluate the biofilm geometry and structure (Downing and Nerenberg, 2008). Here, the biomass volumetric concentration was estimated as $[X] = 5$ mg protein cm^{-3} based on dimensions of the coupon, biofilm depth, and total protein measurements.

Results of a model simulation showing the 2-D profile of DO along the coupon with 5 mM NH_4-T are presented in the SI, Figure S6. The parameter k_{max} was calibrated to the 5 mM NH_4-T DO profile while K_{sn} and K_{so} were kept constant (Fig. 3C). In this case, $NH_3 >> K_{sn}$, making the model insensitive to K_{sn} and allowing k_{max} to be optimized independently. The best fit value for k_{max} of 0.005 μmol mg $protein^{-1}$ s^{-1} was ten-fold lower than the batch k_{max} value of 0.05 μmol mg $protein^{-1}$ s^{-1}. This may be due to inaccuracies in the active biomass density, [X], which has a similar influence on the model as k_{max} and the combined parameter can be represented as $k_{max}X = 0.025$ mol L^{-1} s^{-1}. The biofilm model also assumed that all of the biofilm cells are active, which may not be valid and would effectively reduce [X]. Reducing k_{max} to fit the data can represent a reduction in active biomass, meaning that there may be a smaller fraction of active cells in the biofilm than in a suspended cell culture. Alternatively, k_{max} may in fact be lower in the biofilms than in exponential cells due to lower AMO production.

The suspended cell K_{sn} value of 40 μmol L^{-1} derived from batch experiments was used in the simulations of the biofilm profiles to determine if the affinity of biofilm and suspended cells was similar (Fig. 3B). The model fit to the 1 mM NH_4-T case, where K_{sn} was more significant due to the lower NH_3 concentration, indicates that the K_{sn} derived from batch cells can be used for NH_3 oxidation in biofilms, in this case. The half-saturation constant for oxygen, K_{so}, was assigned a value from the literature and a sensitivity analysis was performed on that value for both 1 and 5 mmol L^{-1} NH_4-T, indicating low sensitivity under these conditions to K_{so} (SI Fig. S7).

The concentration profiles of NH_3 and NO_2^- were also simulated in the 2D RTM (Fig. 3C). The fluxes of these species into and out of the biofilm were used in mass balance calculations to verify that the model accurately simulated the ammonia oxidation reaction. It can also be observed that the NH_3 concentration within the biofilm remains constant with depth, indicating that in a pH buffered medium the equilibrium of NH_3 with NH_4^+ has a buffering effect that results in constant NH_3 concentration even as it is consumed by AOB.

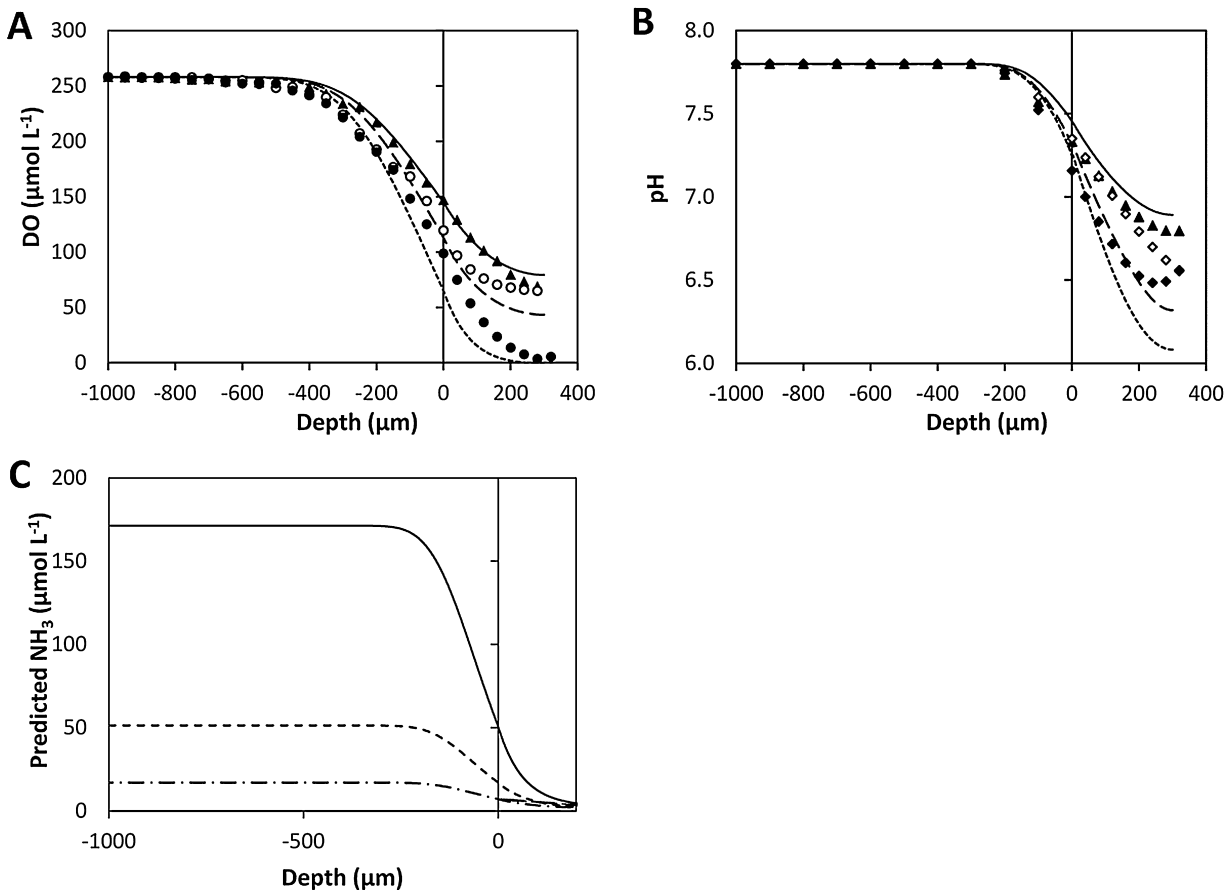

Figure 4. 1-D vertical profiles of DO, pH NH_3, and NO_2^- from Study 1 at a location 2 cm from the inlet DO and pH measured profile data and model results from Study II. Symbols indicate data for 0.5 mM (▲), 1.5 mM (◯), and 5 mM NH_4-T (●). Lines are model results for 0.5 mM (solid), 1.5 mM (long dash), and 5 mM NH_4-T (short dash). **A)** Dissolved oxygen **B)** pH profiles **C)** predicted NH_3 at same location along biofilm length.

In Study I as in the other studies, the model was slightly less accurate fitting the DO concentrations inside the biofilms in comparison to the fluid. This is due to the fluid boundary condition and ability to model the velocity profile with 2-D diffusion. The profile inside the biofilm was more influenced by the reaction rate of AOB, which carries more uncertainty and requires estimation of the Monod kinetic parameters.

Study II—pH Model

The profiles taken in Study II with only 1 mM HEPES buffer confirm that pH gradients develop inside the biofilms when the buffering capacity is low, which correlates with DO consumption by NH_3 oxidation (Fig. 4A and B). Studies of nitrifying biofilm on chalk particles have also shown reduction in pH by the biofilm cells in medium as low as pH 5 (Gieseke et al., 2006). DO concentration with 1.5 and 5 mmol L^{-1} NH_4-T remained higher than in Study I, due to less available NH_3 at lower pH (Fig. 4A).

The 2D biofilm model, with the kinetic parameters derived from the batch model and Study I, was able to simulate the data for both DO and pH (Fig. 4A and B). The simulations indicated that at the same NH_4-T concentrations, NH_3 species concentration was lower in the biofilm in Study II (Fig. 4C) than the simulations of Study I with adequate buffering (Fig. 3C). This difference was due to lower pH with insufficient buffering and a much lower fraction of the total ammonia being present as NH_3.

Study III—K_{sn} Analysis in Biofilms

The goal of the final set of biofilm DO profiles was to evaluate the value of K_{sn} by measuring DO profiles under NH_3-limiting conditions with buffering capacity of Study I. DO was measured in biofilms at concentrations of 0.05, 0.1, 0.25, and 5 mmol L^{-1} NH_4-T (Fig. 5A and C). NH_3 is the limiting substrate at concentrations of 0.1 and 0.05 mmol L^{-1} NH_4-T, as O_2 was not completely consumed (Fig. 5A). At NH_4-T concentrations of 0.25 mmol L^{-1} and higher, the O_2 profiles indicated complete consumption of DO, similar to the 5 mM NH_4-T case in Study I (Fig. 3A).

The model did not fit the DO profiles from Study III well with the k_{max} and K_{sn} used in Study I and II (Fig. 5A). The predicted

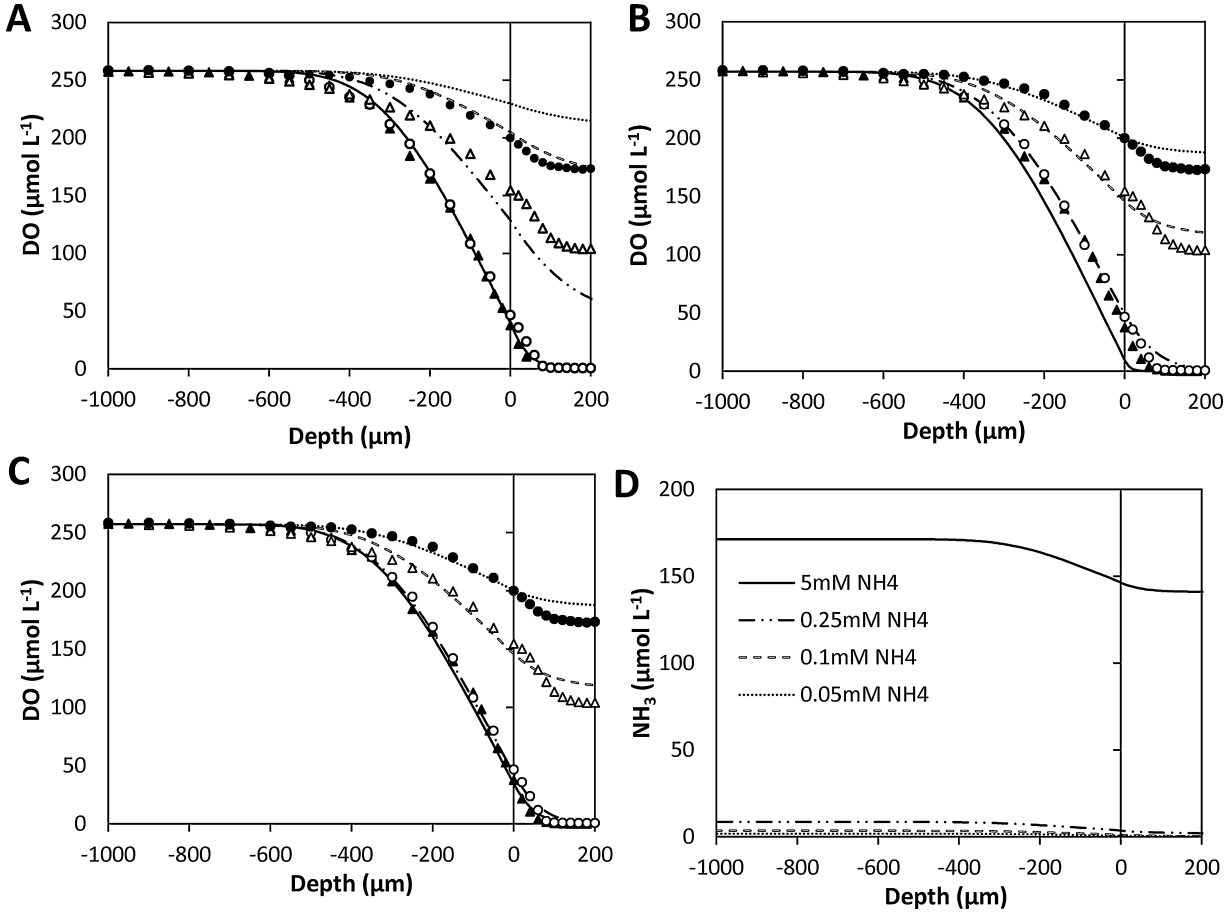

Figure 5. 1-D vertical profiles and corresponding model results of DO, pH and NH_3 from Study III at a location 2 cm from the inlet. Symbols represent measured concentrations of DO in the presence of NH_4-T concentrations of 0.05 (●), 0.1 (Δ), 0.25 (○), and 5 mmol L^{-1} (▲). Lines represent simulations with 0.05 (solid), 0.1 (long dash), 0.25 (dash dot), and 5 (short dash) mmol L^{-1} NH_4-T. (**A**) Data compared to model simulations using Study 1 fitted parameters (Fig. 3): $K_{sn} = 40$ μM NH_3 and $k_{max}X = 0.025$ mol L^{-1} s^{-1}. (**B**) Model simulations with re-fitting $k_{max}X = 0.25$ mol L^{-1} s^{-1}. (**C**) Model simulations with re-fitted parameter $K_{sn} = 4$ μM NH_3 with $k_{max}X = 0.025$ mol L^{-1} s^{-1}. (**D**) Model simulations of NH_3 concentration with depth for re-fitted model parameters in **C**. Error bars represent standard deviation of triplicate profiles.

DO concentrations in the biofilm were higher than the observed data, thus the model under-predicted NH_3 oxidation rates in the biofilms, particularly at low NH_3 concentrations. The $k_{max}X$ parameter was optimized to the 0.05 and 0.1 mM NH_4-T cases, but an accurate fit for all profiles could not be achieved (Fig. 5B). The K_{sn} value was adjusted to obtain optimal least-squares fit to the DO profiles for 0.05 and 0.1 mM NH_4-T. The re-fitting resulted in K_{sn} of 4 μM NH_3, which is 10-fold lower than the value determined in batch experiments and used in Studies I and II (Fig. 5C). With this lower K_{sn} value, all four profiles in Study III were accurately simulated by the model. The better fits could not be obtained by changing the K_{so} due to the high value that would be needed, which did not fit the simulations in Study I (SI, Fig. S7).

The model predicted that NH_3 was completely consumed with 0.05 and 0.1 total NH_4 (Fig. 5D), which confirmed that DO was not the limiting substrate in this case. The simulation of biofilms with low available NH_3 concentration in Study III predicted a lower K_{sn} value of 4 μmol L^{-1}, indicating higher affinity for NH_3 than predicted in Studies I and II, as well as previous work (Suzuki et al., 1974).

The K_{sn} for Study III was not successful in simulating the first two studies with the same values of k_{max} and X (SI, Fig. S8). The biofilms in all three experiments were grown under the same conditions prior to transferring into the experimental chamber. While both the low buffered (Study II) and low NH_3 (Study III) cases resulted in similar DO and NH_3 profiles, the biofilm pH was different in the two cases. The pH dropped to 6.5–6.9 in the Study II biofilm because there was insufficient buffering capacity; but Study III had a constant pH of 7.8 in the biofilm due to the excess HEPES buffer in the fluid. The Monod rate equation used to model ammonia oxidation did not consider pH dependence of the kinetic parameters or nitrite inhibition. These terms can be added in future studies using the same 2D reactive transport model in COMSOL to determine if they are significant.

Conclusions

Microsensors were used in this study to measure O_2 and pH in *N. europaea* biofilms under a range of NH_3 concentrations and buffer concentrations, in order to calibrate an advective transport biofilm model in COMSOL. The advective transport model presented in Equation 1 effectively simulated the advective component of the model. The resulting model was also able to predict the concentration profiles of other aqueous species such as NO_2^- and NH_3. The 2-D model in COMSOL can also be used in other systems with microsensor profiles, where the fluid phase hydrodynamics can be characterized.

The K_{sn} value was initially fitted from the batch data, where K_{so} was insignificant due to constant agitation of batch bottles to ensure adequate oxygen supply. From the data and our sensitivity analyses, it is clear that K_{so} must be very small to drive the oxygen concentrations to zero within a short biofilm depth (Table SI, Fig S7). Although sensitivity analyses were performed on K_{so} to validate the use of a literature value, additional fitting can be done using the model to determine if a more accurate optimal value can be obtained for K_{so}.

Table IV. Kinetic parameters determined with model simulations.

	K_{sn}	K_{so}	k_{max}	X
	μmol L^{-1} NH_3	μmol L^{-1} O_2	μmol NH_3 mg protein^{-1} s^{-1}	mg prot. L^{-1}
Batch model	40	NA	0.05	5.7
Biofilm Study I	40	15.6	0.005	5,000
Biofilm Study II	40	15.6	0.005	4,500
Biofilm Study III	4	15.6	0.005	5,000

In the biofilm Study I, K_{sn} from the batch system was able to simulate the DO profiles, although the resulting k_{max} was much lower than that determined in the batch suspended cell experiments (Table IV). This result could indicate that only a fraction of the biomass in the biofilm was active, or that *N. europaea* cells in a biofilm cannot oxidize NH_3 at the same maximum rate as suspended cells.

The model was able to simulate pH and the impact of acid-base equilibria on AOB activity. This is necessary for nitrification, as the reactions involved produce acid (H^+), which impacts the substrate availability of NH_3. The acid-base equilibria in the model along with the kinetic constants developed in Study 1 were able to model the DO and pH profiles in Study II (Table IV). The model can be used in other kinetic studies of microbial biofilms in environments where both acid-base equilibria and microbial kinetics influence each other. This demonstrates the need to consider acid-base equilibria when evaluating some biofilm catalyzed reactions.

In Study III, NH_3 was the limiting substrate and the fitted K_{sn} value was 4 μmol L^{-1}, which was an order of magnitude lower than the value used in Studies I and II. The dual substrate Monod model used for NH_3 oxidation may result in under prediction of rates when both substrates are at lower concentrations near the K_{sn}. For this reason, it is possible that in the case where neither substrate was replete, a lower K_{sn} for NH_3 was needed to compensate for the rate equation. More investigations of different kinetic equations to describe NH_3 oxidation can be performed using the 2D COMSOL model developed in this work.

This study has shown that a 2-D model can be calibrated to microsensor profiles to determine kinetic parameters of NH_3 oxidation in *N. europaea* biofilms. This model may be used for short term kinetic and inhibition studies of *N. europaea* as well as modified for other single or multispecies biofilms. Future work with this model will include addition of inhibition kinetics to the 2-D model, and comparison with DO profiles of *N. europaea* biofilms during exposure to wastewater contaminants.

We thank the Microsensor group at the Max Planck Institute for Marine Microbiology, Bremen, Germany, for providing microelectrode training. This research was supported by the National Science Foundation with an Integrated Graduate Education and Research Traineeship (IGERT) fellowship (EGL) and NSF Biocomplexity Grant 0412711.

References

Arp DJ,Sayavedra-Soto LA, Hommes NG. 2002. Molecular biology and biochemistry of ammonia oxidation by *Nitrosomonas europaea*. Arch Microbiol 178:(4):250–255.

Bernet N, Sanchez O, Cesbron D, Steyer JP, Delgenes JP. 2005. Modeling and control of nitrite accumulation in a nitrifying biofilm reactor. Biochem Eng J 24:(2):173–183.

Costerton JW, Stewart PS, Greenberg EP. 1999. Bacterial biofilms: A common cause of persistent infections. Science 284:(5418):1318–1322.
Cussler EL. 1997. Diffusion: Mass transfer in fluid systems. 2nd edn. Cambridge: Cambridge University Press.
Downing LS, Nerenberg R. 2008. Effect of oxygen gradients on the activity and microbial community structure of a nitrifying, membrane-aerated biofilm. Biotech Bioeng 101:(6):1193–1204.
Eberl HJ, Sudarsan R. 2008. Exposure of biofilms to slow flow fields: The convective contribution to growth and disinfection. J Theor Biol 253:(4):788–807.
Gieseke A, Bjerrum L, Wagner M, Amann R. 2003. Structure and activity of multiple nitrifying bacterial populations co-existing in a biofilm. Environ Microbiol 5: (5):355–369.
Gieseke A, deBeer D. 2004. Use of microelectrodes to measure in situ microbial activities in biofilms, sediments, and microbial mats. In: Kowalchuk GA, de Bruijn F, Head I, Akkermans A, van Elsas J, editor., Molecular microbial ecology manual. Heidelberg: Springer.
Gieseke A, Tarre S, Green M, de Beer D. 2006. Nitrification in a biofilm at low pH values: Role of in situ microenvironments and acid tolerance. Appl Environ Microbiol 72:(6):4283–4292.
Goeres DM, Hamilton MA, Beck NA, Buckingham-Meyer K, Hilyard JD, Loetterle LR, Lorenz LA, Walker DK, Stewart PS. 2009. A method for growing a biofilm under low shear at the air-liquid interface using the drip flow biofilm reactor. Nat Protoc 4:(5):783–788.
Hyman MR, Arp DJ. 1995. Effects of ammonia on the de novo synthesis of polypeptides in cells of *Nitrosomonas europaea* denied ammonia as an energy source. J Bacteriol 177:(17):4974–4979.
Keener WK, Arp DJ. 1993. Kinetic-studies of ammonia monooxygenase inhibition in *Nitrosomonas europaea* by hydrocarbons and halogenated hydrocarbons in an optimized whole-cell assay. Appl Environ Microbiol 59:(8):2501–2510.
Kreft JU, Picioreanu C, Wimpenny JWT, van Loosdrecht MCM. 2001. Individual-based modelling of biofilms. Microbiol-Sgm 147:2897–2912.
Lauchnor EG, Radniecki TS, Semprini L. 2011. Inhibition and gene expression of *Nitrosomonas europaea* biofilms exposed to phenol and toluene. Biotech Bioeng 108:(4):750–757.
Lazazzera BA. 2005. Lessons from DNA microarray analysis: The gene expression profile of biofilms. Curr Opin Microbiol 8:(2):222–227.
Lide DR. 2007. CRC Handbook of cChemistry and physics. Boca Raton, FL: CRC Press.
Masic A, Bengtsson J, Christensson M. 2010. Measuring and modeling the oxygen profile in a nitrifying Moving Bed Biofilm Reactor. Math Biosci 227:(1):1–11.
Mirpuri R, Jones W, Bryers J. 1997. Toluene degradation kinetics for planktonic and biofilm-grown cells of *Pseudomonas putida* 54G. Biotech Bioeng 53:(6):535–546.
Monds RD, O'Toole GA. 2009. The developmental model of microbial biofilms: ten years of a paradigm up for review. Trends Microbiol 17:(2):73–87.
Okabe S, Naitoh H, Satoh H, Watanabe Y. 2002. Structure and function of nitrifying biofilms as determined by molecular techniques and the use of microelectrodes. Water Sci Technol 46:(1–2):233–241.
Okabe S, Satoh H, Watanabe Y. 1999. In situ analysis of nitrifying biofilms as determined by in situ hybridization and the use of microelectrodes. Appl Environ Microbiol 65:(7):3182–3191.
Park S, Bae W. 2009. Modeling kinetics of ammonium oxidation and nitrite oxidation under simultaneous inhibition by free ammonia and free nitrous acid. Process Biochem 44:(6):631–640.
Park S, Bae W, Rittmann BE. 2010. Multi-Species Nitrifying Biofilm Model (MSNBM) Including Free Ammonia and Free Nitrous Acid Inhibition and Oxygen Limitation. Biotech Bioeng 105:(6):1115–1130.
Perez J, Costa E, Kreft JU. 2009. Conditions for Partial Nitrification in Biofilm Reactors and a Kinetic Explanation. Biotech Bioeng 103:(2):282–295.
Perez J, Picioreanu C, van Loosdrecht M. 2005. Modeling biofilm and floc diffusion processes based on analytical solution of reaction-diffusion equations. Water Res 39:(7):1311–1323.
Radniecki TS, Dolan ME, Semprini L. 2008. Physiological and transcriptional responses of *Nitrosomonas europaea* to toluene and benzene inhibition. Environ Sci Technol 42:(11):4093–4098.
Revsbech NP, Jorgensen BB. 1986. Microelectrodes - Their use in microbial ecology. In: Marshall KC, editor. Adv Microbial Ecology. New York: Plenum Press p 9:293-352.
Riefler RG, Smets BF. 2003. Comparison of a type curve and a least-squared errors method to estimate biofilm kinetic parameters. Water Res 37:(13): 3279–3285.
Rittmann BE, McCarty PL. 2001. Environmental Biotechnology: Principles and Applications. New York: McGraw-Hill.
Robinson RA, Stokes RH. 1959. Electrolyte Solutions. London: Butterworths.
Schramm A, de Beer D, van den Heuvel JC, Ottengraf S, Amann R. 1999. Microscale distribution of populations and activities of *Nitrosospira* and *Nitrospira* spp. along a macroscale gradient in a nitrifying bioreactor: Quantification by in situ hybridization and the use of microsensors. Appl Environ Microbiol 65: (8):3690–3696.
Stein LY, Arp DJ. 1998. Loss of ammonia monooxygenase activity in *Nitrosomonas europaea* upon exposure to nitrite. Appl Environ Microbiol 64:(10):4098–4102.
Stewart PS, Franklin MJ. 2008. Physiological heterogeneity in biofilms. Nat Rev Microbiol 6:(3):199–210.
Suzuki I, Dular U, Kwok SC. 1974. Ammonia or Ammonium Ion as Substrate for Oxidation by *Nitrosomonas-Europaea* Cells and Extracts. J Bacteriol 120: (1):556–558.
Tarre S, Green M. 2004. High-rate nitrification at low pH in suspended- and attached-biomass reactors. Appl Environ Microbiol 70:(11):6481–6487.
Wood B, Quintard M, Whitaker S. 2002. Calculation of effective diffusivities for biofilms and tissues. Biotech Bioeng 77:(5):495–516.
Wood BD, Quintard M, Whitaker S. 2001. Methods for predicting diffusion coefficients in biofilms and cellular systems. In: Doyle RJ, editor. Microbial Growth in Biofilms, Part B: Methods in Enzymology. San Diego, CA: Academic Press. p 319–338.
Yurt N, Beyenal H, Sears J, Lewandowski Z. 2003. Quantifying selected growth parameters of *Leptothrix discophora* SP-6 in biofilms from oxygen concentration profiles. Chem Eng Sci 58:(20):4557–4566.
Zhou XH, Shi HC, Cai Q, He M, Wu YX. 2008. Function of self-forming dynamic membrane and biokinetic parameters' determination by microelectrode. Water Res 42:(10–11):2369–2376.

Supporting Information

Additional supporting information may be found in the online version of this article at the publisher's web-site.